

# Inhibited transesterification and enhanced fibrillation of TLCP by nano-SiO<sub>2</sub> in polycarbonate matrix

Lichuan Wu<sup>a,b</sup>, Peng Chen<sup>a,b</sup>, Jun Zhang<sup>a</sup>, Jiasong He<sup>a,\*</sup>

<sup>a</sup> Key laboratory of Engineering Plastics, Joint Laboratory of Polymer Science and Materials, Institute of Chemistry, Chinese Academy of Sciences, Beijing 100080, China

<sup>b</sup> Graduate School, Chinese Academy of Sciences, Beijing 100039, China

Received 19 May 2005; received in revised form 28 October 2005; accepted 13 November 2005

Available online 1 December 2005

## Abstract

Hybrid composites composed of a thermotropic liquid crystalline polymer (TLCP), nano-SiO<sub>2</sub> and polycarbonate (PC) were prepared by melt blending in a twin-screw extruder. Infrared spectroscopy analysis indicated that the transesterification between PC and TLCP molecules during melt blending was significantly reduced in TLCP/PC blends filled with nano-SiO<sub>2</sub>, compared to the unfilled TLCP/PC one. Scanning electron microscopy (SEM) observation showed that better compatibility and finer TLCP dispersion were reached in the unfilled blend, which made the fibrillation of TLCP difficult in capillary flow even at high shear rate. In contrast to this, well-developed TLCP fibrils were formed by capillary flow in nano-SiO<sub>2</sub> filled TLCP/PC blends. By increasing the nano-SiO<sub>2</sub> concentration and shear rate, the fibrillation of TLCP was significantly enhanced. Thermodynamically the interfacial tension between these components and dynamically the viscosity ratio of TLCP to PC were used to investigate the mechanism of nano-SiO<sub>2</sub> in inhibiting the transesterification and enhancing the fibrillation of TLCP droplets in these hybrid composites.

© 2005 Elsevier Ltd. All rights reserved.

**Keywords:** Transesterification; Nano-SiO<sub>2</sub>; TLCP

## 1. Introduction

During the last two decades, a group of self-reinforced polymer blends, in situ composites consisting of thermoplastics and thermotropic liquid crystalline polymers (TLCPs) attracted an extensive concern, due to TLCP's excellent lubrication during melt processing and potential reinforcing effect for the resultant composites [1–3]. However, the mechanical properties of these composites, relied on the in situ generated TLCP fibrils, are far behind expectations [3]. In recent years, great efforts have been made to improve the mechanical performances as well as lower the cost of in situ composites by using conventional inorganic fillers or fibers additionally [4–11]. Reduced viscosity and improved performances were achieved by filling the TLCP/polysulfone and TLCP/poly (ether ether ketone) in situ composites with carbon fiber [4,5]. Other types of fibres and fillers such as glass fiber (GF), whisker and glass bead (GB) were also used to fill in situ composites by different

research groups [5–12]. Zheng et al. [9,10] found that the presence of GF in the TLCP/polyamide 6 (PA6) in situ composites promoted the fibrillation of TLCP in capillary flow and reduced the viscosity of the composites significantly. Similar results were found by Ding [11] in the study of GB filled TLCP/PA6 composites and by Chen [12] with GB filled TLCP/PC composites. However, these traditional fillers or fibers made the in situ composites much heavier due to their own large density and high loading needed.

Nano-sized particulates filled polymers (nano-composites) are of great interest due to their lower density, excellent performances and attractive prospect, compared to conventionally filled polymers [13,14]. Nano-sized fillers such as carbon black (CB) and nano-SiO<sub>2</sub> have been reported to have unique influence on the morphology of immiscible blends (i.e. phase inversion), especially in conductive materials [15–17]. Recently, it has been reported that nano-fillers such as nano-SiO<sub>2</sub> and nano-clay can also act as a compatibilizer in immiscible blends during mixing process [18–24].

However, there are only a few papers dealing with nano-particles filled in situ composites [25–30]. Hu et al. [25–29] introduced nano-sized fumed silica of different surface properties into the TLCP/polypropylene (PP) in situ blends.

\* Corresponding author. Tel.: +86 10 6261 3251; fax: +86 10 8261 2857.  
E-mail address: [hejs@iccas.ac.cn](mailto:hejs@iccas.ac.cn) (J. He).

They found that hydrophobic nano-SiO<sub>2</sub> could efficiently promote the fibrillation of TLCP droplets by capillary flow or injection molding, resulting in improved mechanical performance of the composites [26]. Chang et al. [30] also reported that only 2 wt% organo-clay could improve the mechanical performance of TLCP/poly (butylene terephthalate) fiber. More recently, Zhang et al. [31] found that nano-clay in the TLCP/PA6 blends had dramatic influences on the dispersion and deformation of TLCP phase. The TLCP droplets got smaller at the clay content of 3 wt%, and deformed into fibrils at the clay content up to 5 and 7 wt%.

In these studies, the fillers changed primarily the physical process occurred during melt processing and physical properties obtained ultimately such as the morphology and mechanical performance of the blends. The influence on chemical process exerted by fillers and the mutual influence between chemical and physical processes during processing have not been reported.

In situ composites consisting of TLCP and thermoplastic polyesters such as PC are especially attractive because of excellent performances of both polymers. For these polyester blends, one of the features is the transesterification during melt blending, by which interfacial adhesion between the components is enhanced and the morphology of blends is changed [32]. It was found that, at short time, the exchange reaction in polyester blends led initially to the formation of block copolymers and as the reaction proceeded, the sequence distribution in the copolyester became statistically random [33]. As a special case reported, the transesterification between PC and TLCP molecules took place easily at temperatures near or above the melt point of TLCP [32,34–37]. This transesterification was determined by many factors such as temperature, concentration and viscosity of components and processing conditions as well. Therefore, it was difficult to control this chemical reaction during processing, which complicated the morphology of the blends [32,37]. On the other hand, TLCP fibrils was unstable and tended to relax or break up at temperatures above the melt point of TLCP, making the fibrillation of TLCP droplets during processing become more difficult [38–42]. For these two reasons, most of the investigation on in situ composites consisting of PC and TLCP were performed at temperatures below the melt point of TLCP. In those cases, TLCP actually did not melt and transesterification could be ignored. As a result, the blends still exhibited high viscosity due to the low processing temperature [43]. Moreover, there is little literature available dealing with the influence of transesterification on the fibrillation of TLCP droplets in TLCP/PC in situ composites [44]. For general understanding, the influence of fillers on the transesterification and subsequently on the fibrillation of TLCP droplets in filled in situ composites is to be investigated.

In the present study, melt blending of TLCP with nano-SiO<sub>2</sub> filled PC and unfilled PC was performed at temperatures above the melt point of TLCP. Transesterification possibly occurring during melt blending process was exploited for nano-SiO<sub>2</sub> filled and unfilled TLCP/PC blends. The morphology of TLCP in these blends was also examined after extrusion at different

shear rates in a capillary rheometer. Selective location of nano-SiO<sub>2</sub> in TLCP/PC blends was analyzed from both thermodynamic and dynamic viewpoints, based on which, the functioning mechanism of nano-SiO<sub>2</sub> in inhibiting the transesterification and enhancing the fibrillation of TLCP droplets in these hybrid composites was discussed in detail.

## 2. Experimental section

### 2.1. Materials

The nano-sized fumed silica (Aerosil R974) used in this work, was purchased from Degussa Co., Germany. Surface modification of the silica with 1,1-dimethyl-dichlorosilane was already performed by the manufacturer. More detailed physical properties of the nano-SiO<sub>2</sub> are listed in Table 1 [45]. A bisphenol A polycarbonate (PC) polymer (Makrolon 3208) was obtained from Bayer Co., Beijing. The melt flow index and density of this resin were 4.5 g/10 min (according to ISO 1133) and 1.2 g/cm<sup>3</sup> (at room temperature), respectively. The commercial thermotropic liquid crystalline polymer (Vectra A950, Hoechst Celanese, USA) employed, was a random copolyester composed of 73 mol% hydroxybenzoic acid and 27 mol% hydroxynaphthoic acid, hereafter labeled as TLCP. Its density was 1.4 g/cm<sup>3</sup>. Its thermal and other properties were described in detail elsewhere [46]. Analytical grade 1,2-dichloroethane was used as the selective solvent for PC.

### 2.2. Sample preparation

All the materials were carefully dried in vacuum at 110 °C for at least 24 h prior to blending. The melt blending was performed using a Haake RC90 Rheocord twin-screw extruder equipped with a pair of counter-rotating intermeshing cone-shaped screws. A temperature profile of 260–275–285–275 °C from hopper to die, respectively, was imposed. The screw speed was 60 rpm. The extrudates were quenched by water and pelletized. To obtain a better dispersion of nano-SiO<sub>2</sub> in the PC matrix, PC/SiO<sub>2</sub> mixtures with varying silica content were pre-extruded, pelletized and well dried, followed by re-extrusion with or without TLCP. The re-extruded pellets were dried again under vacuum at 110 °C for at least 24 h before further use. A fixed TLCP concentration of 10.7 wt% was adopted for all the TLCP/PC containing composites. For convenience of expression, PCSX PCLCPSX are used to label these composites with varying silica content in the following context, where X is assigned to be 0, 1, 3, 5, 10, respectively, referring to the weight percentage of nano-SiO<sub>2</sub> in the pre-filled PC.

Table 1  
Physical properties of nano-SiO<sub>2</sub> R974

Density (g/cm <sup>3</sup> )	BET surface area (m <sup>2</sup> /g)	Average primary particle diameter (nm)	Surface property	Purity (wt% of silica)
2.0	170 ± 20	12	Hydrophobic	> 99.8

### 2.3. Rheological measurements

Rheological measurements were conducted using a Rosand RH7 capillary rheometer (Bohlin Instruments). A capillary die of 1 mm diameter with  $L/D$  of 16 was used. The die entry angle was  $180^\circ$ . The shear viscosities of all well-dried samples at  $285^\circ\text{C}$  were investigated over a wide range of shear rates. The extrudates of blends containing TLCP, obtained at different shear rates from the capillary die, were cooled and collected for morphology observation. Both Bagley and Rabinowitsch corrections were applied for all the data.

### 2.4. Morphology observation

The extrudates from capillary rheometer were cryo-fractured in liquid nitrogen, and sputter-coated with gold. Then, the fracture surface was observed by using a scanning electron microscope (SEM, Hitachi S-4300, Japan). 1, 2-dichloroethane was used to dissolve the matrix resin PC selectively from the samples. TLCP particles and fibrils were separated by centrifuging the solution and decanting the supernatant liquid. This procedure was repeated more than five times. The clean TLCP residue was dried for SEM observation. A software, Photoshop 6.0 was used to measure the diameter of TLCP particles and aspect ratio of fibrils in SEM photographs. At least, 1000 TLCP particles or 300 TLCP fibrils were counted for the statistics of the average diameter or aspect ratio for each sample.

### 2.5. Infrared spectroscopy analysis

Infrared analysis was carried out on a Perkin–Elmer System 2000 FT-IR instrument with a resolution of  $4\text{ cm}^{-1}$ . Wavenumbers between  $400$  and  $4000\text{ cm}^{-1}$  were examined. The blend samples were sufficiently dissolved with 1,2-dichloroethane for at least 48 h, then the soluble and insoluble fractions were carefully separated by ultracentrifugation. The soluble portions were analyzed as thin films obtained by evaporating off solvent. The TLCP, insoluble portion of extracted TLCP/PC blends, was investigated by KBr method. Thin films of neat PC and its physical blend with fine TLCP particles obtained from the previous extraction were also made for comparison. Being carefully controlled, the thickness of all these thin films was in the range of  $80\text{--}100\ \mu\text{m}$ .

## 3. Results and discussion

### 3.1. Inhibition of transesterification between PC and TLCP in nano- $\text{SiO}_2$ filled TLCP/PC blends during extrusion

Transesterification (TE) between PC and Vectra A950 (TLCP) molecules was found to take place readily when they were blended in molten state, by which the compatibility between these components was improved [35–37]. This reaction can be monitored by IR signals of carbonyl groups in the in situ produced block-copolymer molecules [32,35,37].

FT-IR was used here to examine transesterification possibly occurring during melt extrusion for both filled and unfilled

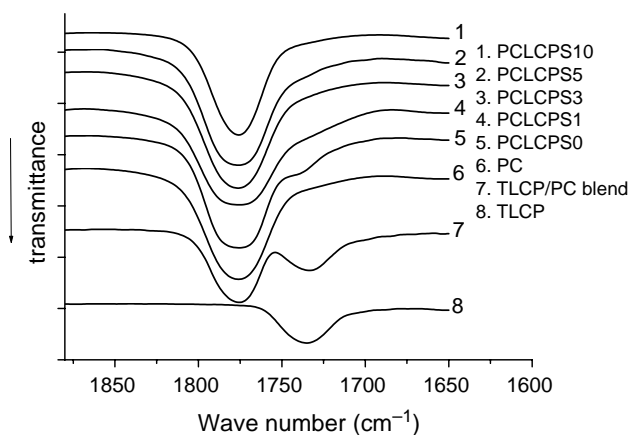


Fig. 1. Fourier transform infrared absorption of carbonyl group in PC, TLCP or their possible copolymer generated in situ by transesterification in blends during processing.

TLCP/PC blends. For comparison, FT-IR spectra of neat PC, TLCP and their physical blend are also given. As shown in Fig. 1, the characteristic signals of carbonyl groups in PC and TLCP molecules locate at  $1780$  and  $1735\text{ cm}^{-1}$ , respectively [32,35]. Both these peaks emerge in the spectrum of TLCP/PC physical blend. However, the spectrum of the soluble fraction of PCLCPS0 shows two signals, the broad peak at about  $1780\text{ cm}^{-1}$  and the other shifted to  $1740\text{ cm}^{-1}$ , respectively, suggesting the in situ formation of a PC-TLCP block-copolymer in this blend during melt processing. The major peak at  $1780\text{ cm}^{-1}$  accounts for PC and the PC blocks in the block-copolymer. The little shoulder around  $1740\text{ cm}^{-1}$ , shifted from  $1735\text{ cm}^{-1}$ , the characteristic signal of neat TLCP, indicates the presence of bound TLCP segments in the copolymer [32,35]. However, this shoulder signal is very weak, indicating that in these blends the amount of TLCP having reacted with the PC matrix was very small. This result is similar to that reported by Costa et al. [47] on reactive blending of polyamide 66 and Vectra A due to short processing time and low concentration of TLCP.

In contrast to the unfilled binary blend, PCLCPS0, the small shoulder around  $1740\text{ cm}^{-1}$  for TLCP segments becomes much weaker and finally disappears in the IR spectra of the soluble fractions of filled blends with nano- $\text{SiO}_2$  loading from 1 to 10 wt%. For PCLCPS1, this little shoulder is much weaker than that of PCLCPS0 and almost unrecognizable, but the curve around  $1740\text{ cm}^{-1}$  appears to show a signal, indicating that transesterification slightly occurred. Further, this little shoulder signal disappears in the spectra corresponding to PCLCPS3, PCLCPS5 and PCLCPS10 composites, meaning no transesterification could be detected. All these results show that even 1 wt% of nano- $\text{SiO}_2$  in PC efficiently inhibited the transesterification between PC and TLCP molecules during melt extrusion at temperatures above the melt point of TLCP.

As another evidence, SEM micrographs (not shown) of cryo-fractured surface of extrudates with varying composition showed that the interface between PC and TLCP phases was changed from obscure in the unfilled one to clear in the nano- $\text{SiO}_2$  filled blends. This suggests the presence of nano- $\text{SiO}_2$  impaired

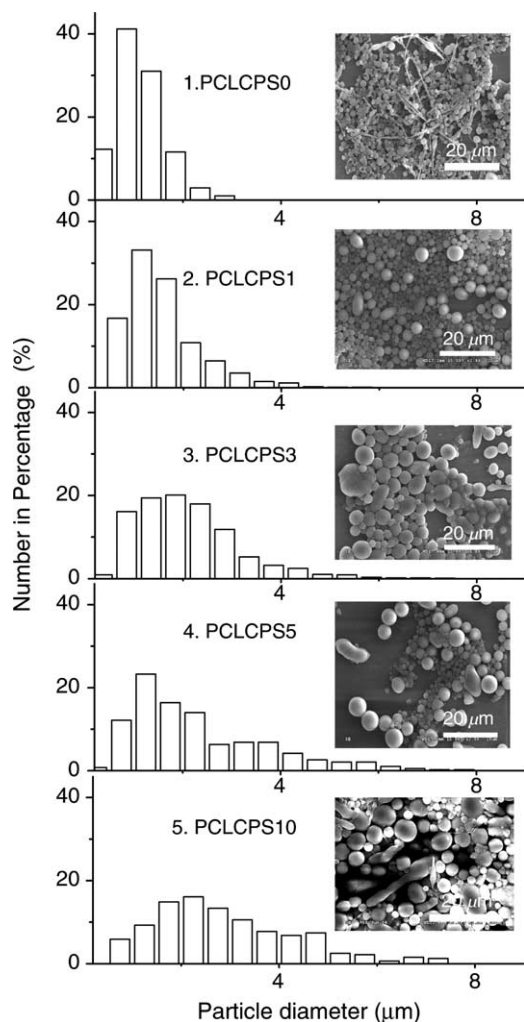


Fig. 2. SEM micrographs and number average diameter size distribution of TLCP particulates with different composition at a shear rate of ca.  $20 \text{ s}^{-1}$ .

the compatibility between PC and TLCP phases in these blends. Naturally, transesterification between PC and TLCP molecules dominated this morphological discrepancy during melt extrusion, since the immiscible pair of PC and TLCP became partially compatible through transesterification [35–37].

Furthermore, the size of the dispersed TLCP particles was used to show the inhibited transesterification between PC and TLCP. According to literature [48–51], reduced compatibility between the TLCP phase and the matrix usually resulted in coarser TLCP particulates. As a result of the present study, Fig. 2 shows frozen morphology of TLCP in blends from capillary flow at a shear rate of ca.  $20 \text{ s}^{-1}$ . For unfilled TLCP/PC blend, PCLCPS0, TLCP particles are fine spherical particles mostly and a small amount of fibrils; whilst for nano-SiO<sub>2</sub> filled blends, TLCP particles are regular spheroids with larger size mainly together with a few ellipsoids. Fig. 2 also gives corresponding diameter distribution of TLCP particles in all the blends. TLCP particles in the PCLCPS0 blend possess the smallest number average diameter of 1.1  $\mu\text{m}$  and the narrowest diameter distribution. In PCLCPS1, the number average diameter of TLCP particles increases up to

1.6  $\mu\text{m}$ , and the diameter distribution becomes a little broader. Further, increasing the concentration of nano-SiO<sub>2</sub> (i.e. PCLCPS3, PCLCPS5 and PCLCPS10) resulted in much larger diameters and broader diameter distributions of TLCP particles. All the FTIR and SEM results indicate that the presence of nano-SiO<sub>2</sub> reduced the compatibility between PC and TLCP, which was usually reached by the transesterification between these two components in melt blending, compared to the unfilled blend. Therefore, the addition of nano-SiO<sub>2</sub> reduced and inhibited the transesterification between PC and TLCP in the filled TLCP/PC blends.

### 3.2. Effect of shear rate on the morphology of TLCP in filled TLCP/PC blends with different nano-SiO<sub>2</sub> contents in capillary flow

The filled and unfilled blends of TLCP/PC were extruded at 285 °C in a capillary rheometer. Influence of the shear rate and nano-SiO<sub>2</sub> concentration on the morphology of TLCP in blends was examined in detail.

Fig. 3 depicts the aspect ratio distribution of TLCP particles for both unfilled and filled TLCP/PC blends at a shear rate of ca.  $240 \text{ s}^{-1}$ . For PCLCPS0, the aspect ratios of about 88% TLCP particles are less than 2 and the remains are larger than 2 and up. For the filled TLCP/PC blends with different nano-SiO<sub>2</sub> loading up to 10 wt%, the amounts of TLCP rods and fibrils increase markedly. Obviously, the presence of nano-SiO<sub>2</sub> in the filled TLCP/PC blends promoted the deformation of the dispersed TLCP droplets into rods and fibrils of larger aspect ratios. This result reveals that in the capillary flow, nano-SiO<sub>2</sub> promoted the deformation of TLCP droplets.

At a high shear rate up to ca.  $1250 \text{ s}^{-1}$ , SEM micrographs of cryo-fractured extrudates and flocculated long fibrils obtained by extraction are shown in Fig. 4, together with the aspect ratio distribution of TLCP particulates and un-flocculated fibrils extracted from all the blends. As shown in the figure, both SEM picture and the statistic value of TLCP aspect ratio indicate only a less than 5% of TLCP fibrils was generated in the unfilled PCLCPS0 blend. However, well-developed TLCP fibrils were observed in the fractured extrudates corresponding to these filled TLCP/PC blends. The higher the nano-SiO<sub>2</sub> concentration was, the better-developed TLCP fibrils were obtained. For each of these filled blends, two portions of unsolvable TLCP particles were obtained after the PC matrix was dissolved selectively by 1,2-dichloroethane: one was composed of rods and fibrils with relatively lower aspect ratios, whose aspect ratio distributions are presented in the bar charts of Fig. 4; and the other of long fibrils flocculating and suspending in the solvent, whose locally magnified micrographs are shown as the insets of these charts. It is clear these fine fibrils were too long to be measured. These data indicate that at a high shear rate, the presence of nano-SiO<sub>2</sub> in blends effectively promoted the deformation of TLCP particles into fibrils, even in the case of only 1 wt% nano-SiO<sub>2</sub> filling, and increasing the nano-SiO<sub>2</sub> concentration increased the aspect ratio of TLCP fibrils, even to mat-like. This further affirms that nano-SiO<sub>2</sub> promoted the deformation and fibrillation of TLCP

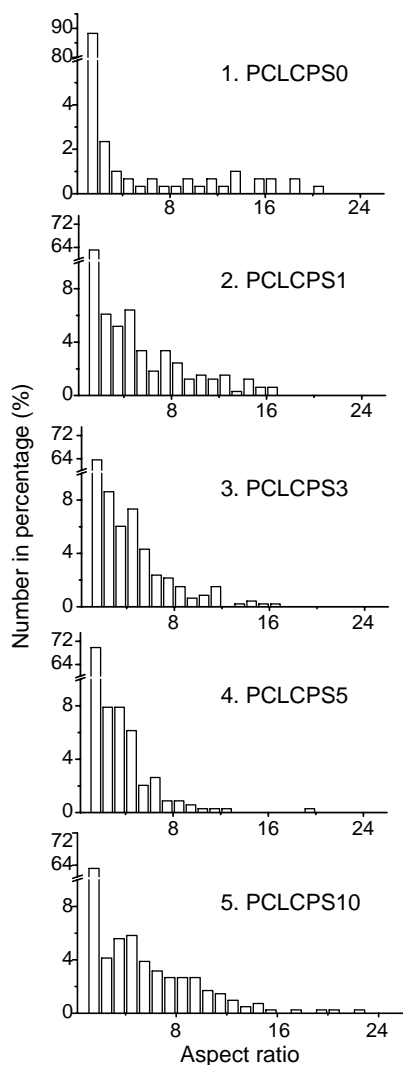


Fig. 3. The dependence of aspect ratio distribution of TLCP particulates on composition at a shear rate of ca.  $240 \text{ s}^{-1}$ .

droplets at temperatures above the melt point of TLCP in the PC matrix by capillary flows.

All these results reveal that in the capillary flow, the deformation and fibrillation of TLCP particles in TLCP/PC binary blend were not sensitive to the shear rate at a relatively high temperature of  $285 \text{ }^\circ\text{C}$ . In contrast, a dramatic change was brought out by adding nano- $\text{SiO}_2$  into the TLCP/PC blends. The deformation of TLCP droplets greatly depended on the shear rate, so that TLCP fibrils of high aspect ratios, even TLCP networks were generated at relatively high shear rates. Moreover, the volume increase of separate particles with increasing shear rate (from a small droplet to a large fibril as shown in Figs. 2 and 4, respectively) in the filled blends indicates the enhancement of flow-induced coalescence of TLCP droplets at high shear rates.

### 3.3. Selective distribution of nano- $\text{SiO}_2$ in TLCP/PC blends

PC and Vectra A950 (TLCP) are thermodynamically immiscible [52]. According to the literature [15–17,53], there

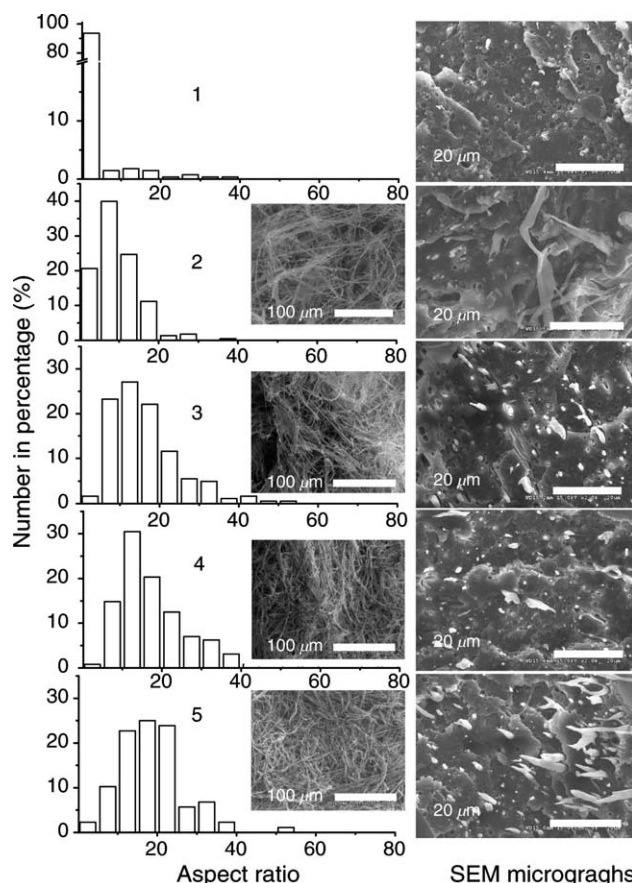


Fig. 4. SEM pictures of cryo-fractured surfaces of extrudates together with corresponding flocculated long fibrils obtained by extraction (the insets), and aspect ratio distribution of TLCP particulates and un-flocculated fibrils extracted for both unfilled and filled TLCP/PC blends at a shear rate of ca.  $1250 \text{ s}^{-1}$ : 1. PCLCPS0; 2. PCLCPS1; 3. PCLCPS3; 4. PCLCPS5; 5. PCLCPS10. Note: for 2–5, the aspect ratio distribution of flocculated long fibrils is not available, due to they are beyond the field of vision in SEM, i.e. too large value to be measured, so that only their SEM micrographs are presented.

would be three possibilities of distribution for nano- $\text{SiO}_2$  in the filled TLCP/PC blends: (1) nano- $\text{SiO}_2$  distributed exclusively in PC; (2) nano- $\text{SiO}_2$  was encapsulated by the dispersed TLCP; (3) nano- $\text{SiO}_2$  retained at the interface of PC and TLCP. It has been reported that the selective distribution of nano-scaled fillers imposed great influence on the morphology of immiscible polymeric blends [15–20]. So it is necessary to know the distribution of nano- $\text{SiO}_2$  in filled TLCP/PC blends. In practical processing, the filler distribution is determined by thermodynamic parameters (e.g. the interfacial tension between polymers or between polymer and filler) and dynamic parameters (e.g. the viscosity of component polymers) [15,54–58].

#### 3.3.1. Selective filling of nano- $\text{SiO}_2$ in TLCP/PC blends by thermodynamic driving force

Premphet and Horanont [57] found that in filled blends composed of a pair of immiscible polymers the filler distributed selectively in the polymer-phase, by which it possessed the lowest interfacial tension. Sumita et al. extended this

qualitative approach further [54] and introduced a wetting coefficient,  $W_a$ , which was used to predict the selective distribution of filler:

$$W_a = \frac{\gamma_{\text{filler-B}} - \gamma_{\text{filler-A}}}{\gamma_{\text{A-B}}} \quad (1)$$

where,  $\gamma_{\text{filler-A}}$  and  $\gamma_{\text{filler-B}}$  are the interfacial tensions between the filler and polymer A or B, respectively, and  $\gamma_{\text{A-B}}$  is the interfacial tension between polymer A and B. If  $W_a > 1$ , the filler distributes within A-phase; if  $-1 < W_a < 1$ , the filler is located at the interface; if  $W_a < -1$ , the filler is selective for the B-phase.

In the present study, the interfacial tension between PC and TLCP was calculated according to harmonic mean equation of Wu [59,60]:

$$\gamma_{\text{A-B}} = \gamma_A + \gamma_B - \frac{4\gamma_A^d \gamma_B^d}{\gamma_A^d + \gamma_B^d} - \frac{4\gamma_A^p \gamma_B^p}{\gamma_A^p + \gamma_B^p} \quad (2)$$

where  $\gamma_A$  and  $\gamma_B$  are the surface energy of two polymers A and B in contact, and the superscripts d and p denote the dispersion and polar components of the surface energy. Here, A is PC and B is TLCP.

For calculation of the interfacial tensions between filler and polymers, the geometric mean equation of Wu [59] was used, which was more practicable for systems composed of a high-energy material such as nano-SiO<sub>2</sub> and a low-energy material such as a polymer:

$$\gamma_{\text{A-B}} = \gamma_A + \gamma_B - 2(\gamma_A^d \gamma_B^d)^{1/2} - 2(\gamma_A^p \gamma_B^p)^{1/2} \quad (3)$$

In this case, A refers to PC or TLCP, and B to nano-SiO<sub>2</sub>. Corresponding values of the surface energy taken from literatures [61–63] are listed in Table 2.

According to Eqs. (2) and (3), the values of interfacial tensions  $\gamma_{\text{PC-TLCP}}$ ,  $\gamma_{\text{PC-Silica}}$  and  $\gamma_{\text{TLCP-Silica}}$  are listed in Table 3. It shows that the interfacial tension between the silica and PC,  $\gamma_{\text{PC-Silica}}$  approximates the corresponding value between the silica and TLCP,  $\gamma_{\text{TLCP-Silica}}$ . According to Refs. [57,64], this means approximate affinity for nano-SiO<sub>2</sub> to TLCP coils and to PC melt in the blends. The value of the wetting coefficient also confirmed this tendency. Eq. (1) yielded a wetting coefficient of 0.02. In the filled TLCP/PC blends, nano-SiO<sub>2</sub> initially dispersed in PC tended to migrate to the interface between the TLCP melt droplet and PC matrix due to equivalent interfacial tensions between PC and nano-SiO<sub>2</sub>, and between TLCP and nano-SiO<sub>2</sub>, respectively.

Table 2  
Surface tension of polymers and nano-silica [61–63]

	Surface tension (mN/m)		
	Total $\gamma$	Disperse component ( $\gamma^d$ )	Polar component ( $\gamma^p$ )
PC <sup>a</sup>	40.48	29.67	10.81
TLCP	35.69	31.09	4.61
Nano-SiO <sub>2</sub> <sup>b</sup>	81.7	72.3	9.5

<sup>a</sup> Calculated from Ref. [61].

<sup>b</sup> Values of nano-SiO<sub>2</sub> with almost the same size and surface properties [63].

Table 3  
Interfacial tension between the possible polymer–polymer and polymer–filler pairs

Possible pairs	Interfacial tensions (mN/m)
$\gamma_{\text{PC-TLCP}}$	2.53
$\gamma_{\text{PC-Silica}}$	9.28
$\gamma_{\text{TLCP-Silica}}$	9.33

### 3.3.2. Selective filling of nano-SiO<sub>2</sub> in TLCP/PC blends by dynamic driving force

The distribution of filler in a blend composed of immiscible polymers is also determined dynamically by viscosity discrepancy of two polymers, when these two polymers possess approximate affinity to the filler, according to the results of Persson et al. [55,56]. In their study, they found that the aluminum borate whiskers distributed in the high viscosity polyisobutylene (PIB) phase except when they promoted coherency of the low viscosity minority polyethylene (PE) phase. Furthermore, they discovered that if PIB was just slightly more viscous, the slightly higher surface energy of PE still ruled the absorption of whiskers. Interestingly, Benderly et al. obtained a similar result from their investigation of GF (or GB) filled PA/PP blends [58].

In our present study, PC and TLCP had the approximate affinity to the nano-SiO<sub>2</sub>, while the viscosity of polycarbonate was higher than that of TLCP over the entire range of shear rate investigated, which was expressed in the form of viscosity ratio (the viscosity of dispersed TLCP,  $\eta_d$  to the viscosity of PC matrix,  $\eta_m$ ) versus shear rate as shown by the circles in Fig. 5. The viscosity ratio of TLCP to PC decreases rapidly from 0.83 to 0.17 with shear rate accordingly increasing from 20 to 2200 s<sup>-1</sup>. According to Persson's study, the nano-SiO<sub>2</sub> dynamically tended to migrate to the polycarbonate melt with increasing shear rate.

Dominated by these two factors discussed above, the distribution of nano-SiO<sub>2</sub> varied with the shear rate. At relatively low shear rates, the viscosity difference of these two polymers was small and the interfacial tension dominated the selective distribution of nano-SiO<sub>2</sub>, making it located at the interface between PC and TLCP phases. While at relatively high shear rates, the viscosity difference of these two polymers enlarged and became predominant, resulting in the migration of nano-SiO<sub>2</sub> from the TLCP/PC interface to the vicinity of PC.

### 3.4. Mechanism analysis

All the above results indicate that for the filled TLCP/PC blends, transesterification readily occurred in the unfilled TLCP/PC blend was efficiently suppressed during melt blending and well-developed TLCP fibrils were generated by capillary flow at appropriate shear rates. This suggested that nano-SiO<sub>2</sub> particles dominated the suppressed transesterification and increased fibrillation of TLCP. Therefore, based on both the experimental results and theoretical calculation of selective distribution of nano-SiO<sub>2</sub> in TLCP/PC blends, a mechanism analysis is necessary for better understanding of these two processes.

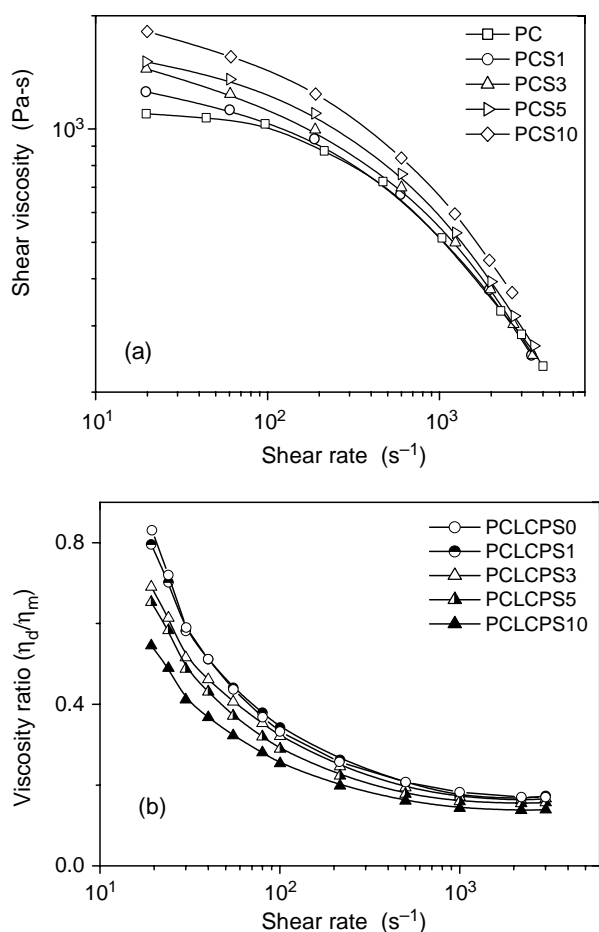


Fig. 5. Shear rate dependence of viscosity or viscosity ratio for nano-SiO<sub>2</sub> filled composites with various filler loadings at 285 °C: (a) PC/SiO<sub>2</sub> composites; (b) TLCP/SiO<sub>2</sub>/PC composites.

### 3.4.1. Inhibition of transesterification between PC and TLCP by nano-SiO<sub>2</sub> in filled PC

According to above analysis, nano-SiO<sub>2</sub> particles tended to locate at the TLCP/PC interface, driven by the interfacial tension in the TLCP/PC blends at appropriate shear rates. Therefore, transesterification between PC and TLCP phases was easily hindered by nano-SiO<sub>2</sub> particles. To clarify further the role of nano-SiO<sub>2</sub> in restraining the transesterification between PC and TLCP molecules, a schematically quantitative calculation for surface coverage ratio of TLCP droplets is presented in Table 4. Here, the average diameters of nano-silica spheres, 12 nm and TLCP particulates, 1.0 μm, were used for the quantitative calculation. It was supposed that the whole surface of TLCP droplets was accessible for nano-SiO<sub>2</sub> particles. Obviously, a considerable surface coverage ratio of 120% (more than a single-layer) for TLCP droplets was obtained even in the case of 0.0055 volume fraction of nano-SiO<sub>2</sub> added for PCLCPS1 composite. Actually, practical coverage ratio was usually lower than the calculated value due to the existence of nano-SiO<sub>2</sub> aggregates. Hence, it was still possible for transesterification to occur, as shown in Fig. 1. In the case of PCLCPS3 composite, the quantity of nano-SiO<sub>2</sub> particles was enough to cover the whole surface of TLCP droplets by more than three single-layers. Further, much

Table 4  
Quantitative analysis of surface coverage for TLCP droplets by nano-SiO<sub>2</sub> particles

Composites	TLCP (vol%)	Nano-SiO <sub>2</sub> (vol%)	Particle concentration ratio $N_{\text{SiO}_2}/N_{\text{TLCP}}$ (number per unit volume)	Surface coverage ratio of TLCP droplets by nano-SiO <sub>2</sub> (%)
PCLCPS0	9.31	0	0	0
PCLCPS1	9.35	0.55	$3.4 \times 10^4$	120
PCLCPS3	9.42	1.65	$1.0 \times 10^5$	360
PCLCPS5	9.49	2.77	$1.7 \times 10^5$	610
PCLCPS10	9.66	5.65	$3.4 \times 10^5$	1220

thicker covering layers of nano-SiO<sub>2</sub> were available for both PCLCPS5 and PCLCPS10 composites. Consequently, the opportunity for collision between PC and TLCP molecules in ternary blends reduced remarkably, and then transesterification was readily depressed. These calculated results agreed well with the previous FTIR analysis: the transesterification was reduced significantly in PCLCPS1 composite and almost inhibited completely in composites with increasing silica content. Similar situation was reported by Vermant et al. [20] when they investigated the coalescence suppression in model immiscible polymer blends composed of polydimethylsiloxane (PDMS) and polyisobutylene (PIB) by nano-SiO<sub>2</sub> particles after a pre-shearing at high shear rate. They found that the coalescence of dispersed PIB droplets was efficiently slowed down or suppressed completely by adding 0.5 or 1 wt% nano-SiO<sub>2</sub>, which located at the TLCP/PC interface or had a little better affinity to the PDMS continuous phase. In the present study, nano-SiO<sub>2</sub> stayed at the interface between the TLCP and PC domains suppressed the transesterification, instead of the coalescence of TLCP droplets.

### 3.4.2. Influence of nano-SiO<sub>2</sub> distribution on fibrillation of TLCP droplets in TLCP/PC blends

**3.4.2.1. Influence of viscosity ratio on fibrillation of TLCP droplets in TLCP/PC blends.** It is commonly known that the deformation of TLCP droplets is governed by several factors, including the viscosity ratio between components, concentration of TLCP, miscibility between components and processing conditions [3,65,66]. For a specified system and given processing condition, the viscosity ratio of the dispersed TLCP to the thermoplastic matrix is of great importance in determining the fibrillation of TLCP for in situ composites [65,66]. Usually, the lower the viscosity ratio below unity is, the better-developed TLCP fibrils are achieved for TLCP/PC blends in extrusion or injection molding process at relatively low temperatures [65–68]. Hu et al. [25,26] found that hydrophobic nano-SiO<sub>2</sub> could effectively promote the fibrillation of TLCP droplets for TLCP/PP blends both in capillary flow and injection molding. And they claimed that nano-SiO<sub>2</sub> acted as a viscosity thickening agent lowering the viscosity ratio. Fig. 5(a) depicts the effect of nano-SiO<sub>2</sub> content on the viscosity of PC/SiO<sub>2</sub> composites over a wide range of shear rates. For the composites with low filler loading, only a slight

increase of viscosity was observed at relatively high shear rates, suggesting that viscosity change caused by nano-SiO<sub>2</sub> in these composites can be ignored. Correspondingly, Fig. 5(b) gives curves of the viscosity ratio versus shear rate for both unfilled and filled TLCP/PC blends. In the latter case, PC/SiO<sub>2</sub> was regarded as an entity for the matrix phase, according to Hu et al. [25]. The viscosity ratio of TLCP to PC/SiO<sub>2</sub> reduced little for TLCP/SiO<sub>2</sub>/PC composites with low nano-SiO<sub>2</sub> loading, compared with TLCP/PC at the same shear rate. At high shear rates, the values of viscosity ratio at the same shear rate were almost the same for both TLCP/PC blend and TLCP/SiO<sub>2</sub>/PC composites. Moreover, as shown in Fig. 1, the transesterification in the TLCP/PC binary blend was very limited due to the low concentration of TLCP and short processing time, which suggested that the change of molecular weight (or viscosity macroscopically) of the components resulted from the transesterification could be ignored. Therefore, the viscosity ratio of TLCP to the matrix (or equivalent medium) was not the predominant factor determining the fibrillation of TLCP in this study. There was some new possible mechanism dominant for TLCP/SiO<sub>2</sub>/PC composites, other than the viscosity thickening mechanism put forward by Hu et al. in the TLCP/SiO<sub>2</sub>/PP composites [25]. Obviously, by considering the small size and shape of nano-SiO<sub>2</sub> particles, this novel mechanism was also distinct from others such as the instantaneous capillaries mechanism formed by GF in the TLCP/GF/PA composites [10] and the dynamic micro-roll mechanism generated by GB in TLCP/GB/PA composites [11], respectively.

*3.4.2.2. Influence of nano-SiO<sub>2</sub> distribution on fibrillation of TLCP droplets in TLCP/PC blends.* According to Ding [11] and Hu [29], the selective distribution of fillers was of great importance in determining the deformation of TLCP droplets in TLCP/GB/PA and TLCP/SiO<sub>2</sub>/PP composites. For these systems, GB or nano-SiO<sub>2</sub> located exclusively in one polymer phase. However, in the present study, the distribution of nano-SiO<sub>2</sub> tended to show a dependence on the shear rate: at relatively low shear rates, nano-SiO<sub>2</sub> particles located at the TLCP/PC interface, driven by the interfacial tension and suppressing the transesterification; at relatively high shear rates, enlarged viscosity disparity between TLCP and PC tended to make nano-SiO<sub>2</sub> particles migrate from the TLCP/PC interface to PC matrix. As a result, the selective distribution of nano-SiO<sub>2</sub> particles promoted the fibrillation of TLCP droplets in capillary flow in two ways. One is the depressed transesterification by nano-SiO<sub>2</sub> reduced the miscibility and weakened the interfacial adhesion between PC and TLCP phases, increased the mobility and enhanced the collision probability, thereby enhanced the coalescence of TLCP droplets [3]. The other is the migration of nano-SiO<sub>2</sub> particles from the TLCP/PC interface to PC matrix driven by the dynamic force, favored the collision (thereby coalescence) of TLCP droplets in the capillary flow. This migration made nano-SiO<sub>2</sub> act as an accelerant rather than a depressor for the coalescence of TLCP droplets [18,19]. Consequently, nano-SiO<sub>2</sub> in filled TLCP/PC blends enhanced the coalescence

and fibrillation of TLCP droplets by shearing and elongation (at the entrance of the capillary die) actions in capillary flow, when the shear rate was high enough [42,65,68].

#### 4. Conclusions

Transesterification between PC and TLCP molecules in the TLCP/PC composites during melt blending was effectively suppressed by pre-filling PC matrix with nano-SiO<sub>2</sub> particles, resulting in clear interface between components. This reaction was significantly reduced even at down to 1 wt% nano-SiO<sub>2</sub> loading. Increasing the content of nano-SiO<sub>2</sub> led to almost complete inhibition of this reaction. Moreover, in contrast to the unfilled TLCP/PC blend, well-developed TLCP fibrils were obtained in the successive capillary flow by raising the shear rate for the filled TLCP/PC blends with nano-SiO<sub>2</sub> content from 1 to 10 wt%. Increasing both the nano-SiO<sub>2</sub> content and shear rate improved the fibrillation of TLCP droplets significantly. These phenomena were ascribed to the selective distribution of nano-SiO<sub>2</sub> in PC and TLCP phases, driven by the interfacial tension thermodynamically and the viscosity discrepancy of components dynamically. During melt blending, the interfacial tension dominated the selective distribution of nano-SiO<sub>2</sub> at the TLCP/PC interface and suppressed the transesterification. And then, the increased shear rate enlarged the viscosity disparity between TLCP and PC, thus made nano-SiO<sub>2</sub> particles migrate from the TLCP/PC interface to PC matrix, enhanced the mobility of TLCP phase, promoted the coalescence and the subsequent fibrillation of TLCP droplets in capillary flow. This mechanism of nano-SiO<sub>2</sub> in Vectra A950/PC blends was different from that in LC5000/PP blends proposed by Hu et al. [25].

#### Acknowledgements

This work was supported by the National Nature Science Foundation of China, Grant No. 50233010.

#### References

- [1] Kiss G. *Polym Eng Sci* 1987;27:410–23.
- [2] Qin YM. *Polym Adv Technol* 1996;7:151–9.
- [3] Tjong SC. *Mater Sci Eng* 2003;R41:1–60.
- [4] He J, Zhang H, Wang Y. *Polymer* 1997;38:4279–83.
- [5] He JS, Wang YL, Zhang HZ. *Compos Sci Technol* 2000;60:1919–30.
- [6] Tjong SC, Meng YZ. *Polymer* 1999;40:1109–17.
- [7] Tjong SC, Meng YZ. *Polymer* 1999;40:7275–83.
- [8] Shumsky VF, Getmanchuk IP, Lipatov YS. *J Appl Polym Sci* 2000;76:993–9.
- [9] Zheng X, Zhang B, Zhang J, Xue Y, He J. *Int Polym Process* 2003;18:3–11.
- [10] Zheng XJ, Zhang J, He JS. *J Polym Sci, Part B: Polym Phys* 2004;42:1619–27.
- [11] Ding YF, Zhang J, Chen P, Zhang BQ, Yi ZQ, He JS. *Polymer* 2004;45:8051–8.
- [12] Chen P, Zhang J, He J. *Polymer* 2005;18:7652–7.
- [13] Ray SS, Okamoto M. *Prog Polym Sci* 2003;28:1539–641.
- [14] Rong MZ, Zhang MQ, Zheng YX, Zeng HM, Friedrich K. *Polymer* 2001;42:3301–4.
- [15] Steinmann S, Gronisk W, Friedrich C. *Polymer* 2002;43:4467–77.



- [16] Gubbels F, Blacher S, Vanlathem E, Jerome R, Deltour R. *Macromolecules* 1995;28:1559–66.
- [17] Gubbels F, Jerome R, Vanlathem E, Deltour R, Blacher S, Brouers F. *Chem Mater* 1998;10:1227–35.
- [18] Zhang Q, Yang H, Fu Q. *Polymer* 2004;45:1913–22.
- [19] Vermant J, Cioccolo G, Nair KG, Moldenaers P. *Rheol Acta* 2004;43:529–38.
- [20] Wang Y, Zhang Q, Fu Q. *Macromol Rapid Commun* 2003;24:231–5.
- [21] Voulgaris D, Petridis D. *Polymer* 2002;43:2213–8.
- [22] Khatua BB, Lee DJ, Kim HY, Kim JK. *Macromolecules* 2004;37:2454–9.
- [23] Ray SS, Pouliot S, Bousmina M, Utracki LA. *Polymer* 2004;45:8403–13.
- [24] Ray SS, Bousmina M. *Macromol Rapid Commun* 2005;26:450–5.
- [25] Lee MW, Hu X, Yue CY, Li L, Tam KC, Nakayama KJ. *Appl Polym Sci* 2002;86:2070–8.
- [26] Lee MW, Hu X, Yue CY, Li L, Tam KC. *Compos Sci Technol* 2003;63:339–46.
- [27] Lee MW, Hu X, Li L, Yue CY, Tam KC, Cheong LY. *Compos Sci Technol* 2003;63:1921–9.
- [28] Zhang L, Tam KC, Gan LH, Yue CY, Lam YC, Hu X. *J Appl Polym Sci* 2003;87:1484–92.
- [29] Lee MW, Hu X, Li L, Yue CY, Tam KC. *Polym Int* 2003;52:276–84.
- [30] Chang IH, Seo BS, Kim SH. *J Polym Sci, Part B: Polym Phys* 2004;42:3667–76.
- [31] Zhang B, Ding Y, Chen P, Liu C, Zhang J, He J, Hu G. *Polymer* 2005;46:5385–95.
- [32] Porter RS, Wang LH. *Polymer* 1992;33:2019–29.
- [33] Devaux J, Godard P, Mercier JP. *J Polym Sci, Part B: Polym Phys* 1982;20:1881–94.
- [34] Wei KH, Ho JC. *Macromolecules* 1997;30:1587–93.
- [35] Tovar G, Carreau PJ, Schreiber HP. *Colloids Surf A* 2000;161:213–23.
- [36] Kil SB, Park OO, Yoon KH. *J Appl Polym Sci* 1999;73:2123–33.
- [37] Kil SB, Park OO, Yoon KH. *J Appl Polym Sci* 2001;82:2799–807.
- [38] Tan LP, Joshi SC, Yue CY, Lam YC, Hu X, Tam KC. *Acta Mater* 2003;51:6269–76.
- [39] Tan LP, Yue CY, Tam KC, Lam YC, Hu X, Nakayama K. *J Polym Sci, Part B: Polym Phys* 2003;41:2307–12.
- [40] Chan HS, Leng Y, Gao F. *Compos Sci Technol* 2002;62:757–65.
- [41] Machiels AGC, VanDam J, DeBoer AP, Norder B. *Polym Eng Sci* 1997;37:1512–25.
- [42] Filipe S, Cidade MT, Wilhelm M, Maia JM. *Polymer* 2004;45:2367–80.
- [43] Turek DE, Simon GP, Tiu C. *Polym Eng Sci* 1995;35:52–63.
- [44] Engberg K, Stromberg O, Martinsson J, Gedde UW. *Polym Eng Sci* 1994;34:1336–45.
- [45] Saint-Michel F, Pignon F, Magnin A. *J Colloid Interface Sci* 2003;267:314–9.
- [46] Sauer BB, Kampert WG, McLean RS. *Polymer* 2003;44:2721–38.
- [47] Costa G, Meli D, Valenti B, Falqui L. *Polymer* 2001;42:8035–42.
- [48] Seo Y, Hong SM, Kim KU. *Macromolecules* 1997;30:2978–88.
- [49] Datta A, Baird DG. *Polymer* 1995;36:505–14.
- [50] Huang G, Chan PK, Kamal MR. *Can J Chem Eng* 2003;81:243–57.
- [51] Zhang H, Weiss RA, Kuder JE, Cangiano D. *Polymer* 2000;41:3069–82.
- [52] Hsieh TT, Tiu C, Hsieh KH, Simon GP. *J Appl Polym Sci* 2000;77:2319–30.
- [53] Zoldan J, Siegmann A, Narkis M. *J Polym Eng* 2003;23:119–48.
- [54] Sumita M, Sakata K, Asai S, Miyasaka K, Nakagawa H. *Polym Bull* 1991;25:265–71.
- [55] Benderly D, Siegmann A, Narkis M. *J Polym Eng* 1997;17:461–89.
- [56] Persson AL, Bertilsson H. *Polymer* 1998;39:5633–42.
- [57] Premphet K, Horanont P. *Polymer* 2000;41:9283–90.
- [58] Benderly D, Siegmann A, Narkis M. *Polym Compos* 1996;17:86–95.
- [59] Wu S. *Polymer interface and adhesion*. vol. 1. New York: Marcel Dekker; 1982.
- [60] Wu S. *Polym Eng Sci* 1987;27:335–45.
- [61] Hobbs SY, Dekkers MEJ, Watkins VH. *Polymer* 1988;29:1598–602.
- [62] Ma K, Chung TS, Good RJ. *J Polym Sci, Part B: Polym Phys* 1998;36:2327–37.
- [63] Ou YC, Yu ZZ. *Rubber Chem Technol* 1994;67:834–44.
- [64] Schuster RH, Issel HM, Peterseim VI. *Rubber Chem Technol* 1996;69:769–80.
- [65] Beery D, Kenig S, Siegmann A. *Polym Eng Sci* 1991;31:451–8.
- [66] He JS, Bu WS, Zhang HZ. *Polym Eng Sci* 1995;35:1695–704.
- [67] Sukhadia AM, Done D, Baird DG. *Polym Eng Sci* 1990;30:519–26.
- [68] He JS, Bu WS. *Polymer* 1994;35:5061–6.